

JPL



Future directions in volcano remote sensing

Paul Lundgren
*Jet Propulsion Laboratory
California Institute of Technology*

Motivation

Volcano deformation: complex variations in space/time

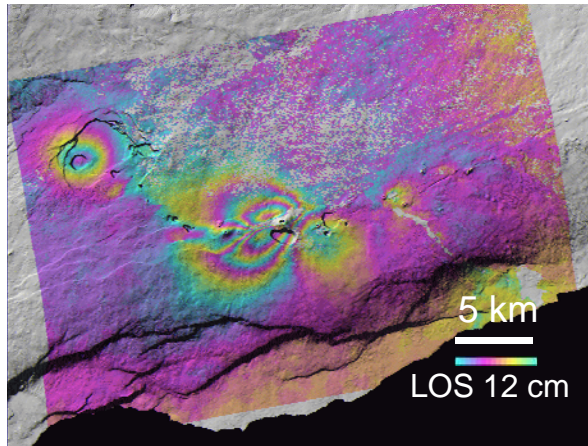


Figure 1-1. Deformation of June 2007 Eruption, Kilauea volcano from L-band ALOS InSAR (processing by Z. Lu).

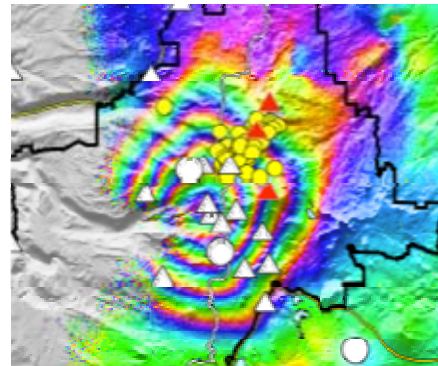
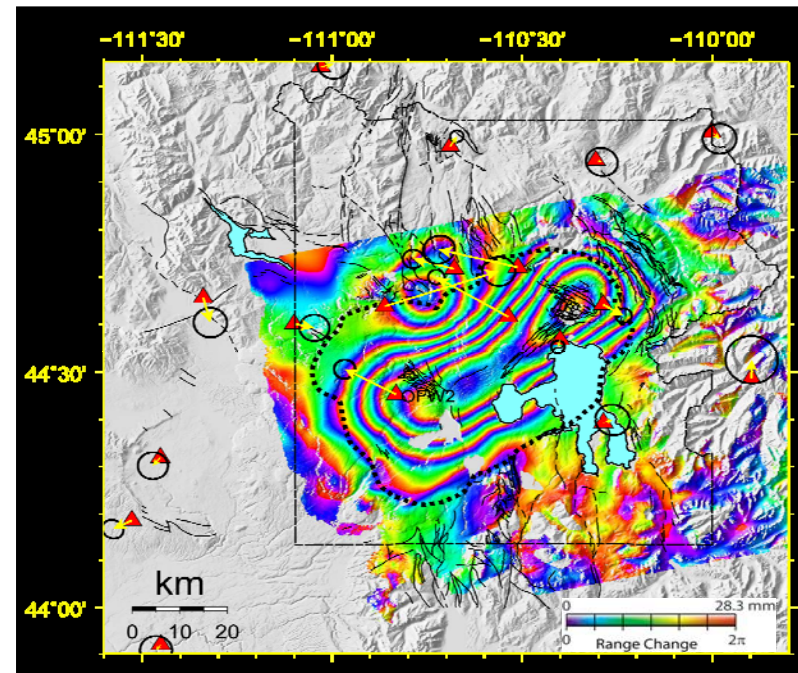


Figure 1-3. Satellite SAR interferogram for Three Sisters (red triangles) group showing the differential interferogram spanning the 1996-2000 time interval. Each 'fringe' is 2.83 cm in the satellite line-of-sight (LOS). Deformation source represents an inflationary source (sill, *Wicks et al., 2002*) that first began to deform in 1996.

Figure 1-6. **Yellowstone** caldera InSAR observation from the sum of two interferograms spanning the 2004-2006 time period (2004-2005 and 2005-2006) showing uplift (large area within caldera) and subsidence (circular fringes on NW rim of caldera) that requires a complex set of sources and magma flow from beneath the center of the caldera [*Wicks et al., in preparation, 2007*].





Outline

- Radar wavelength
L-band
- Deformation resolution
High spatial sampling, ~20m,
cm-level over 30 km distance
Need for even denser sampling → near
surface, small spatial processes (dome
dikes)
- Spatial coverage
Normal 40-100km swath
- Revisit time → rapid eruption processes
Sub-weekly repeat pass
Atmospheric issues
- Mission duration → long-term processes
5 year nominal

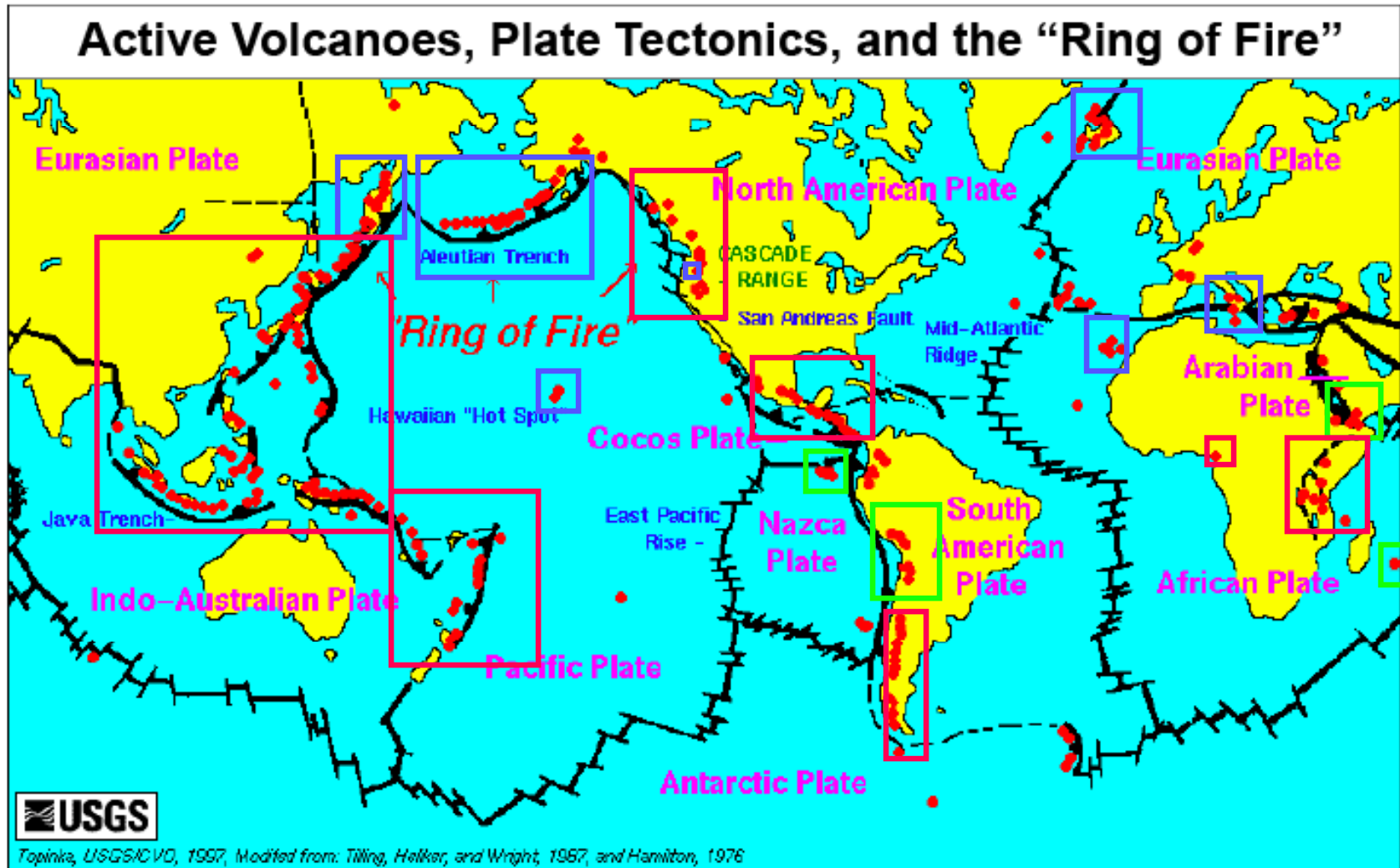


Some science objectives

- Simply characterizing deformation and other RS signals over the broad time spectrum of volcano processes
- Understanding magma migration from depth
- Understanding dynamic processes
- Differences across a broad spectrum of volcano types (chemistry) and activity

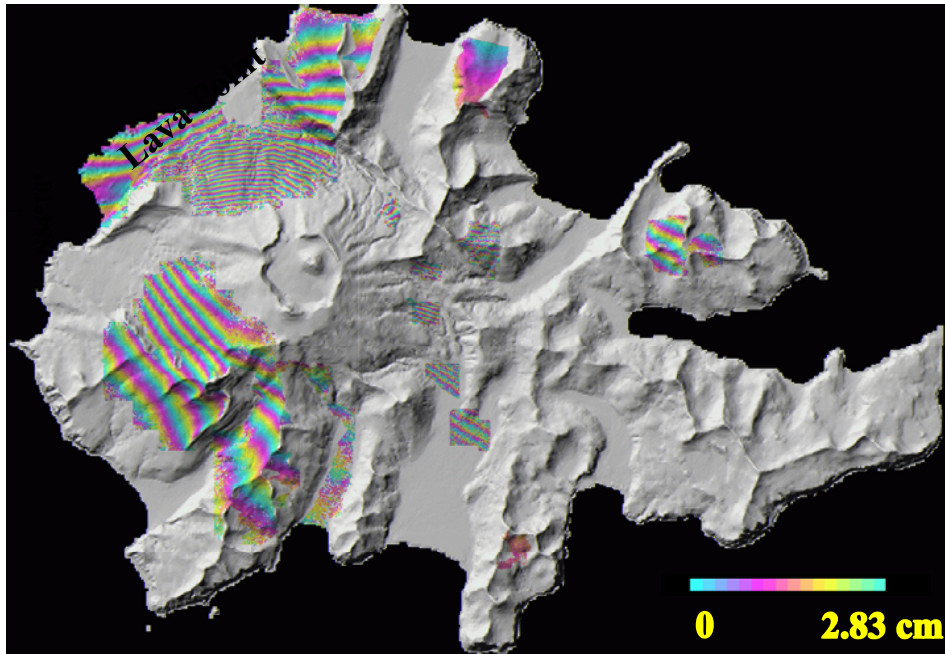
C-band InSAR volcano effectiveness

excellent
 Works – better with L-band
 Bad - but good for L-band?

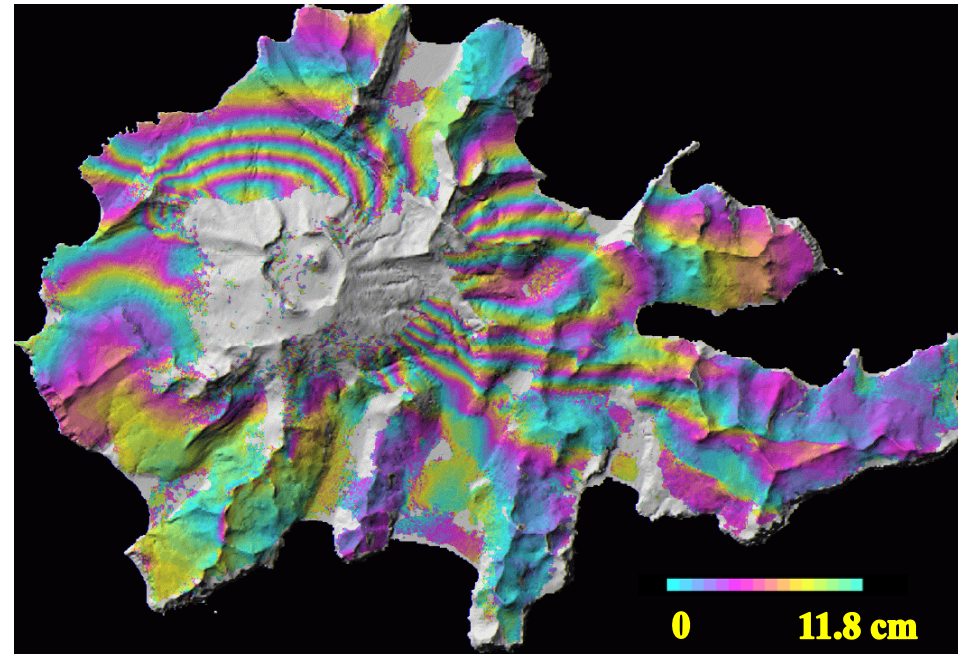


C-band vs L-band Akutan, Aleutians

Deformation mapped by ERS
(C-band, $\lambda = 5.66$ cm) InSAR



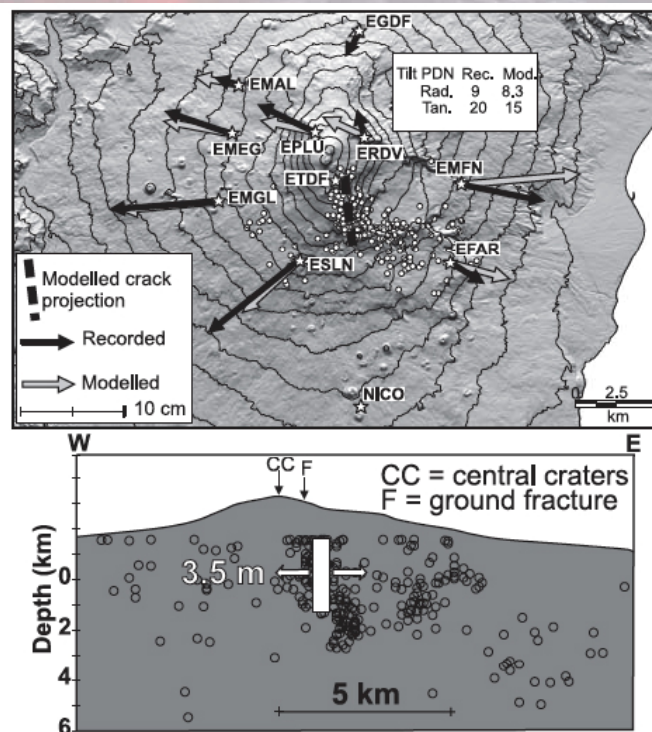
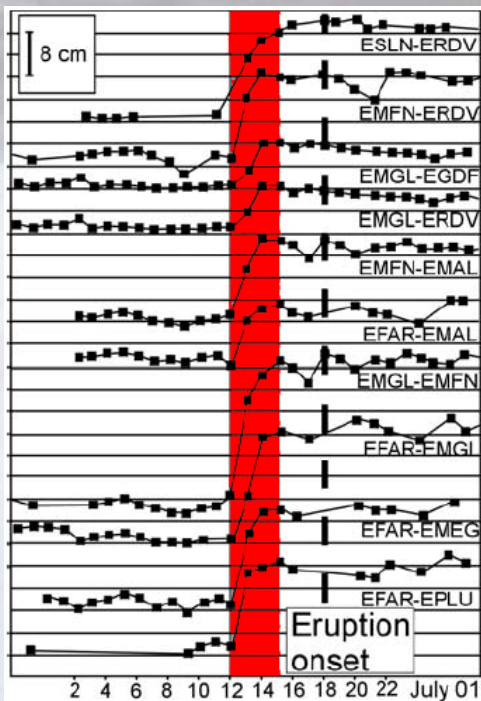
Deformation mapped by JERS
(L-band, $\lambda = 23.53$ cm) InSAR



Courtesy Zhong Lu, USGS

Time and spatial scales: Etna 2001 eruption example

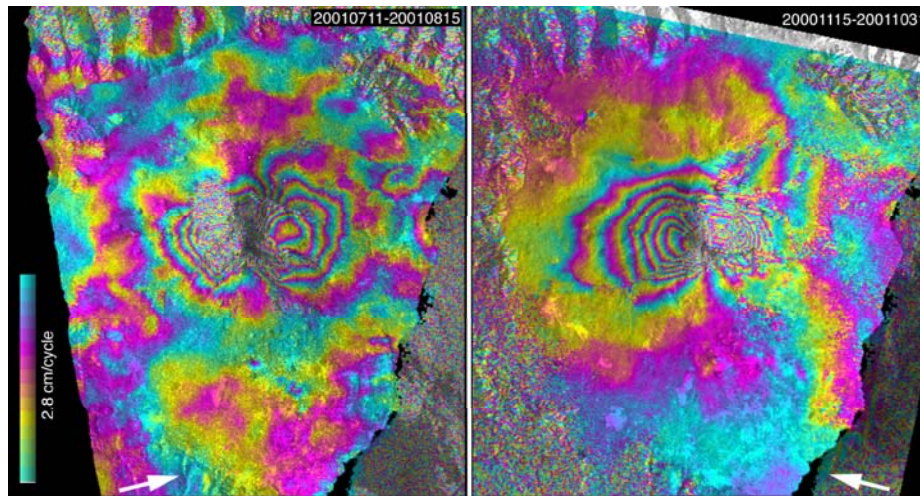
GPS data shows large dike went from 3 km b.s.l to 3 km summit within a few days, all within 7 days of large flank eruption



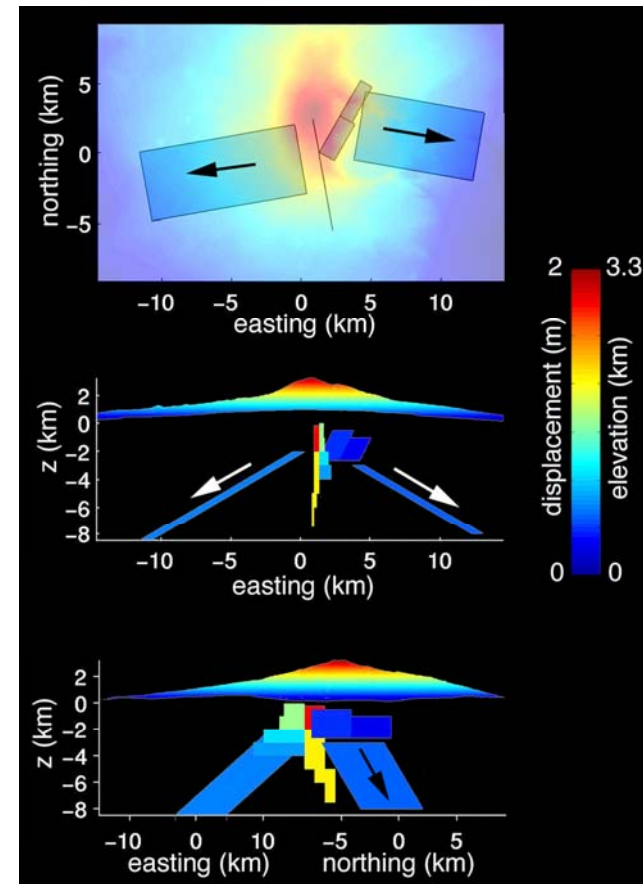
Cont. GPS baselines, and modeled source (Bonaccorso et al., GRL 2002)

Bonaccorso, A., M. Aloisi, and M. Mattia (2002), Dike emplacement forerunning the Etna July 2001 eruption modeled through continuous tilt and GPS data, *Geophys. Res. Lett.*, 29(13), 1624, 10.1029/2001GL014397.

InSAR provides new discoveries, but temporal sampling inadequate



Ascending and descending data constrain source geometry, 1 month and 1 year interferograms do not constrain time evolution



Lundgren and Rosen, *Geophys. Res. Lett.*, 2003

InSAR observations of Etna 2001 eruption

Dense spatial sampling constrain source mechanisms

Short repeat time needed for dike propagation Example from the Galapagos

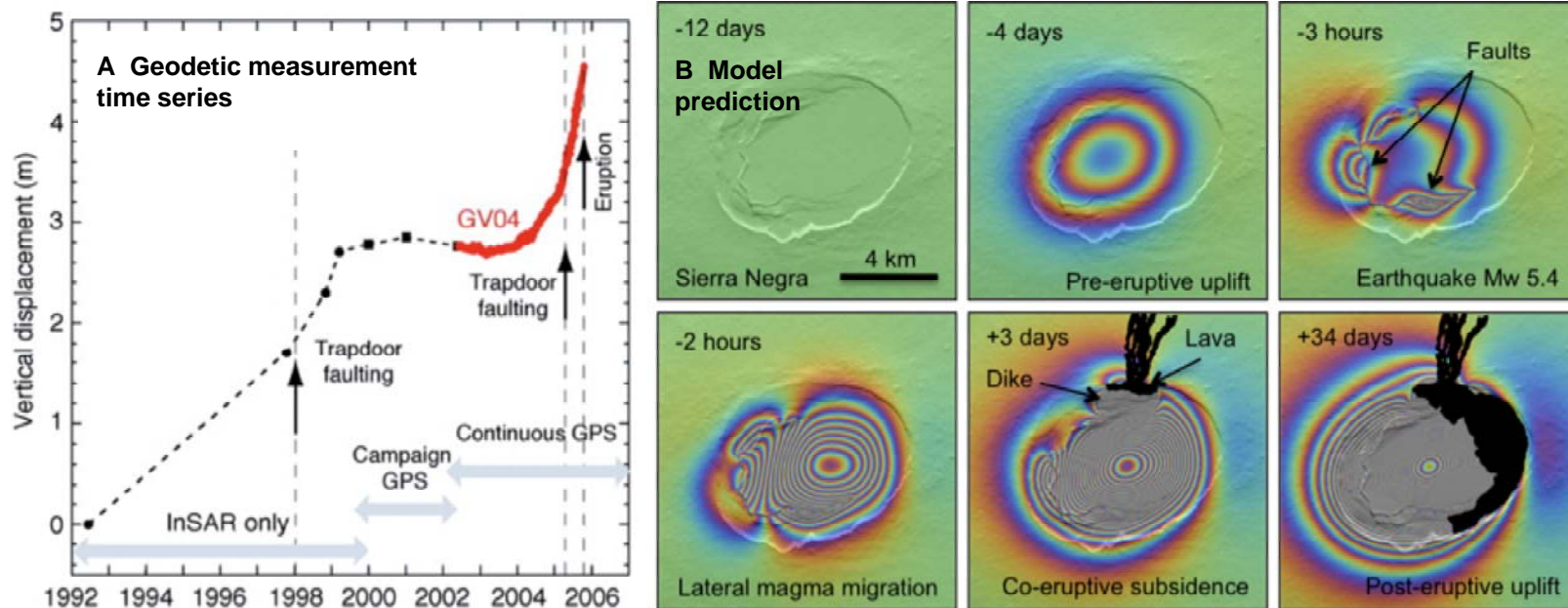
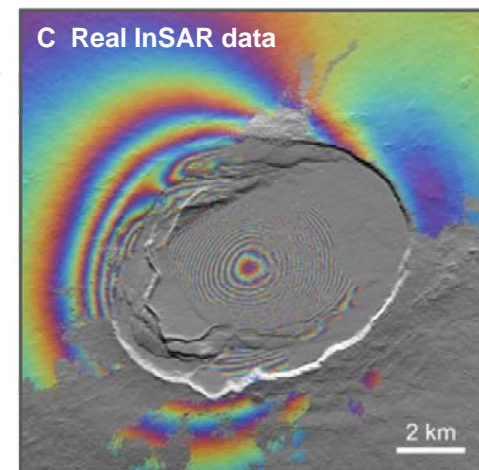


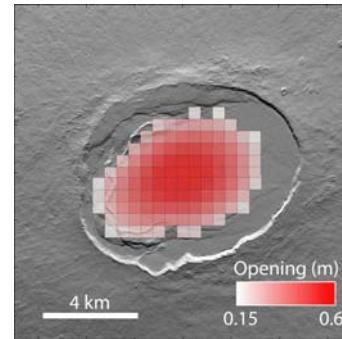
Figure 1-2. VESPA will provide temporal resolution comparable to that of a point GPS measurement (the red line in A), but with InSAR's spatial resolution (B) to capture the pre-eruptive transient deformation. (A) Uplift history of the caldera center of Sierra Negra volcano, Galapagos, constructed by InSAR and GPS measurements [Chadwick et al., 2006]. (B) Simulated interferograms of deformation events around the onset of the 2005 eruption of the volcano, based on InSAR, GPS, seismic data, and fieldwork observations combined [Yun, 2007]. An earthquake (Mw 5.4) occurred three hours prior to the eruption, which induced lateral magma migration and dike intrusion that fed the eruption. (C) Envisat satellite InSAR data where all the intermediate stages of the transient deformation were not observed.



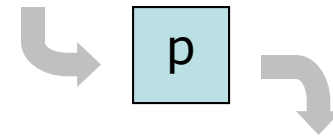
Courtesy Sang-Ho Yun, JPL

Adjusting InSAR using GPS

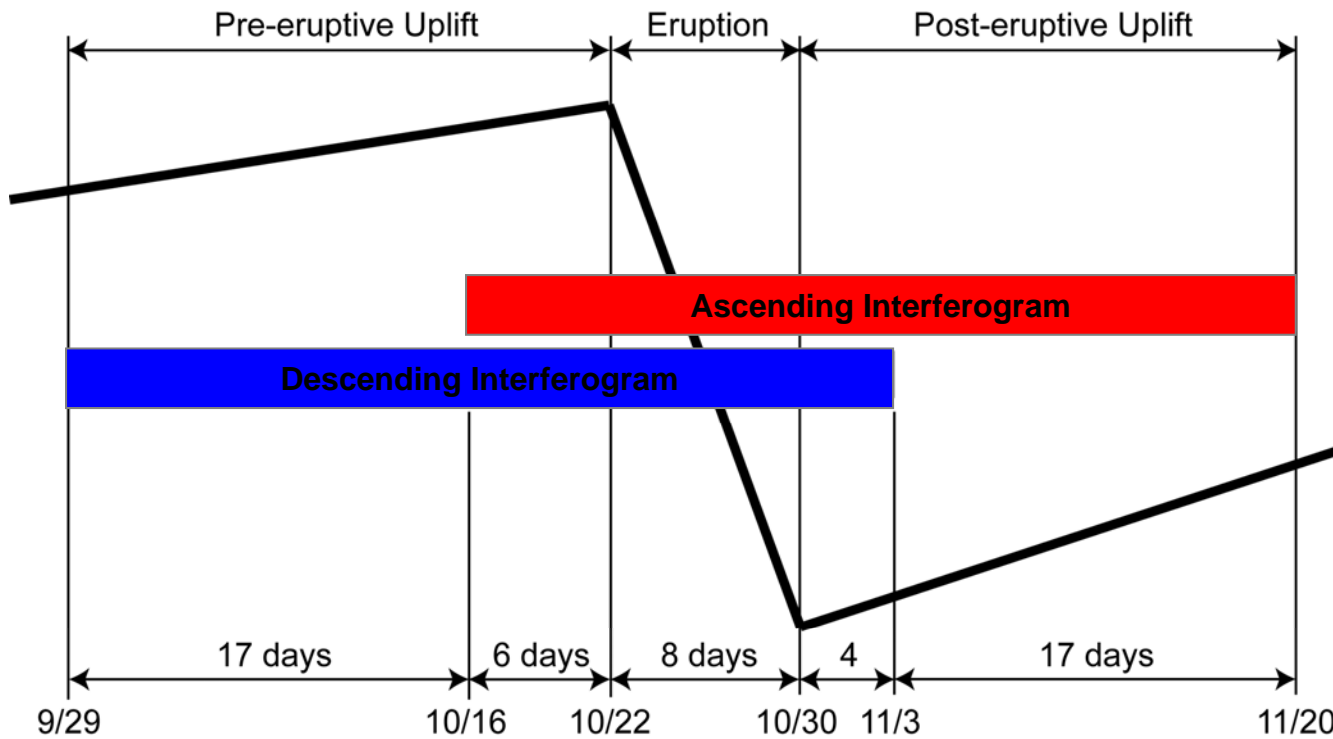
Galapagos (cont'd)
 Courtesy S. Yun



$$\begin{aligned}
 s &= Bp \\
 u &= Gs \\
 \Delta x_{t2} - \Delta x_{t1} &= Du
 \end{aligned}$$



$$\begin{aligned}
 s &= Bp \\
 d_{\text{InSAR}} &= G's
 \end{aligned}$$





1. Pre-eruptive inflation

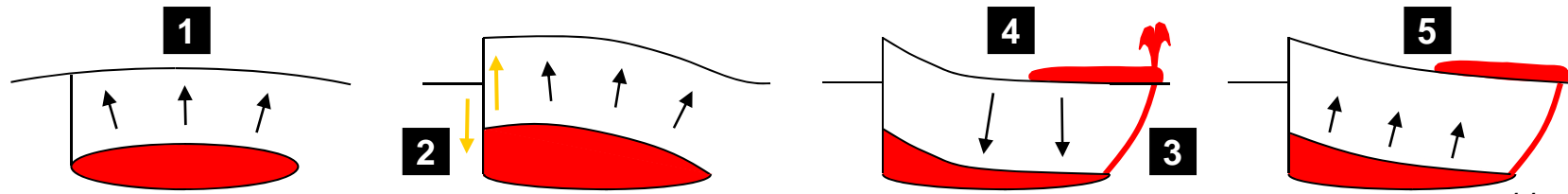
2. Faulting

- Earthquake (Mw 5.4) 3 hrs prior to the eruption
- Fresh fault scarp along the sinuous ridge (Chadwick & Geist, personal comm.)

3. Dike intrusion

4. Co-eruptive subsidence

5. Post-eruptive inflation



Galapagos (cont'd) courtesy S. Yun

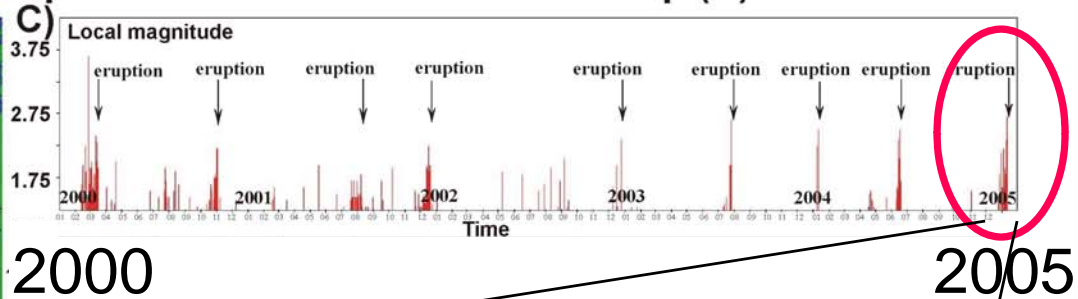
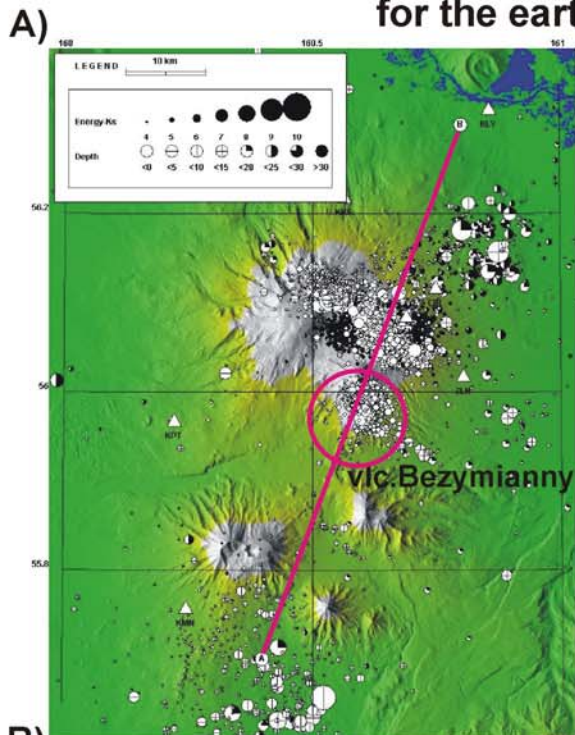
JPL



Eruption time scales *Bezymianny lava dome*

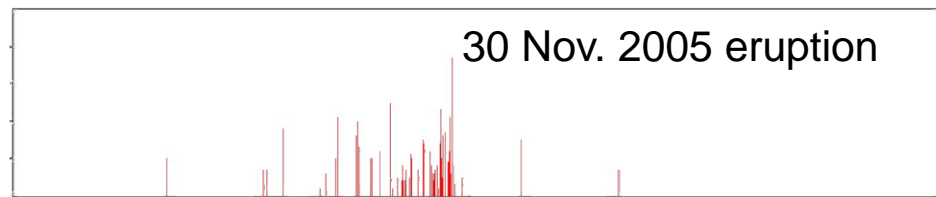
ASTER V-SWIR-TIR

Seismicity of Bezymianny volcano from January 2000 to February 2005: map (A), vertical cross-section (B), graphs of seismic activity (C-F) for the earthquakes located within circle at map (A)



2000

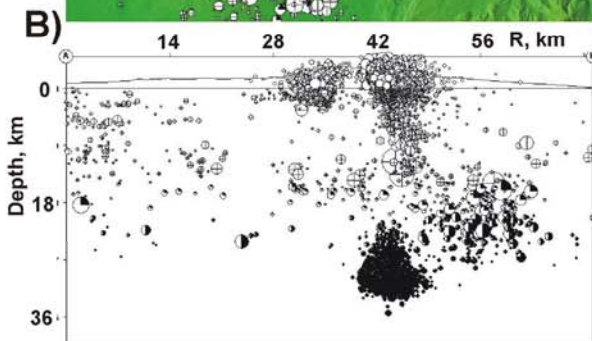
2005



2 months

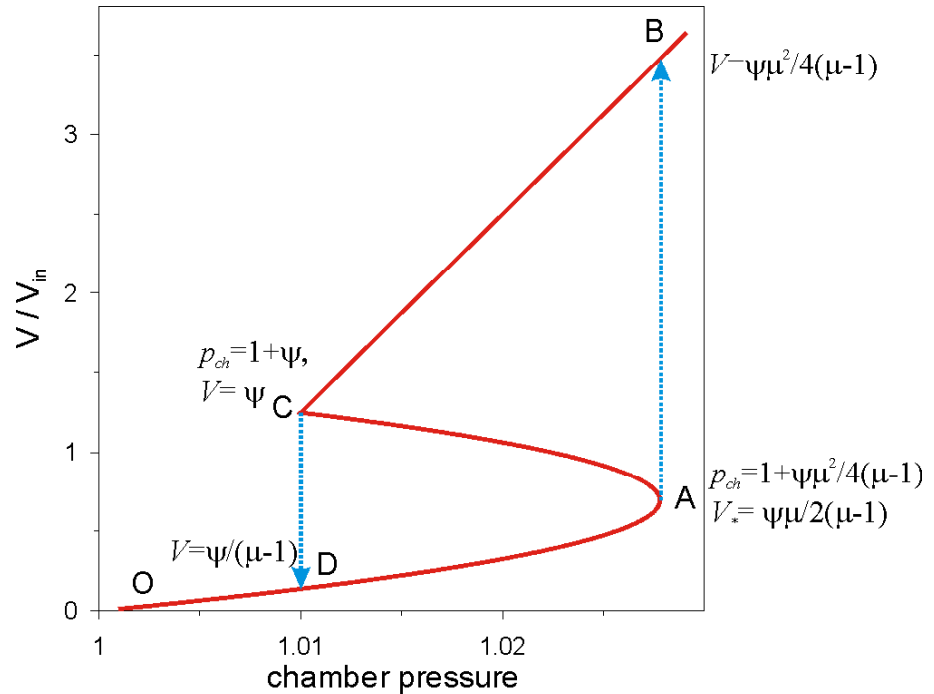
For large eruptions, seismicity shows that weekly or shorter revisit times are required to track pre-eruptive deformation

courtesy Sergey Senyukov, Kamchatkan Branch of Geophysical Survey, Petropavlovsk-Kamchatskiy, Russia



Dynamic volcano models require high spatial temporal sampling

Steady-state periodic dome growth and eruption models



Melnik and Sparks, Nature, 1999

Barmin et al., EPSL, 2002

Mason et al., JVGR, 2006

Figures courtesy Oleg Melnik



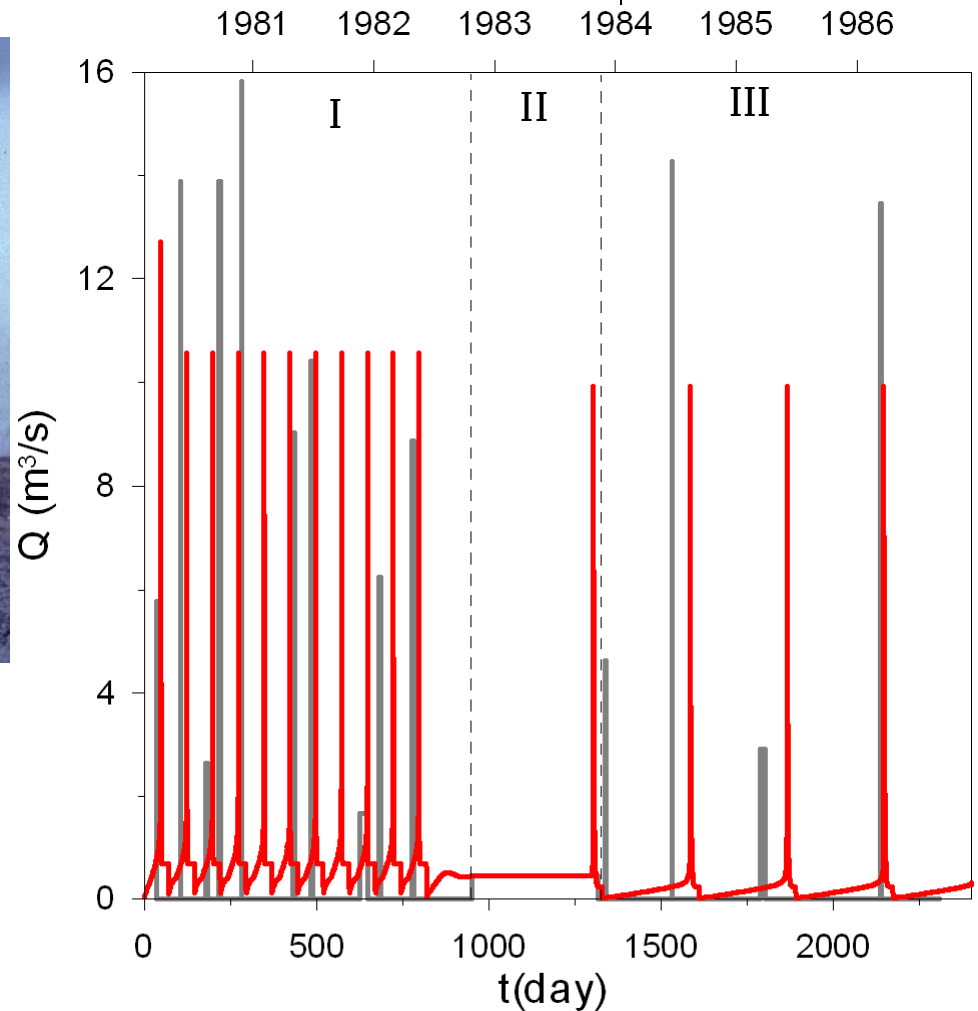
Mount St Helens (1980-1987)

3 periods of dome growth;

I - 9 pulses $\sim 12 \text{ m}^3\text{s}^{-1}$, $Q_{av}=0.67 \text{ m}^3\text{s}^{-1}$

II - continues, $Q_{av}=0.48 \text{ m}^3\text{s}^{-1}$

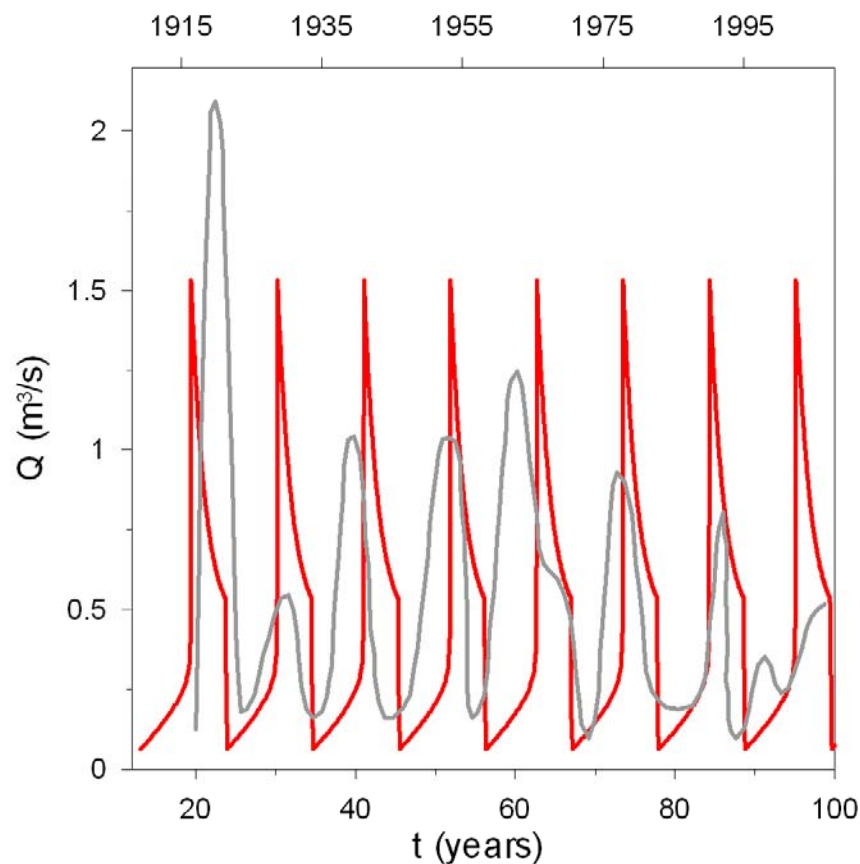
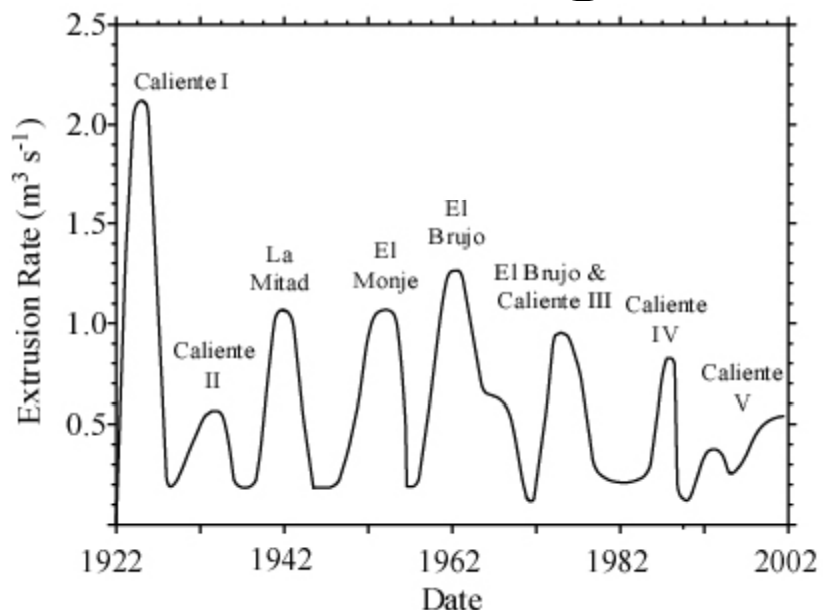
III- 5 pulses $< 15 \text{ m}^3\text{s}^{-1}$, $Q_{av}=0.23 \text{ m}^3\text{s}^{-1}$



Courtesy Oleg Melnik

Santiaguito

Cycles: 8 after 1922
 high ($0.5-2.1 \text{ m}^3 \text{ s}^{-1}$): 3-6-years
 low ($\leq 0.2 \text{ m}^3 \text{ s}^{-1}$): 3-11-years
 Average discharge: $\sim 0.44 \text{ m}^3 \text{ s}^{-1}$



Courtesy Oleg Melnik

Long-term deformation

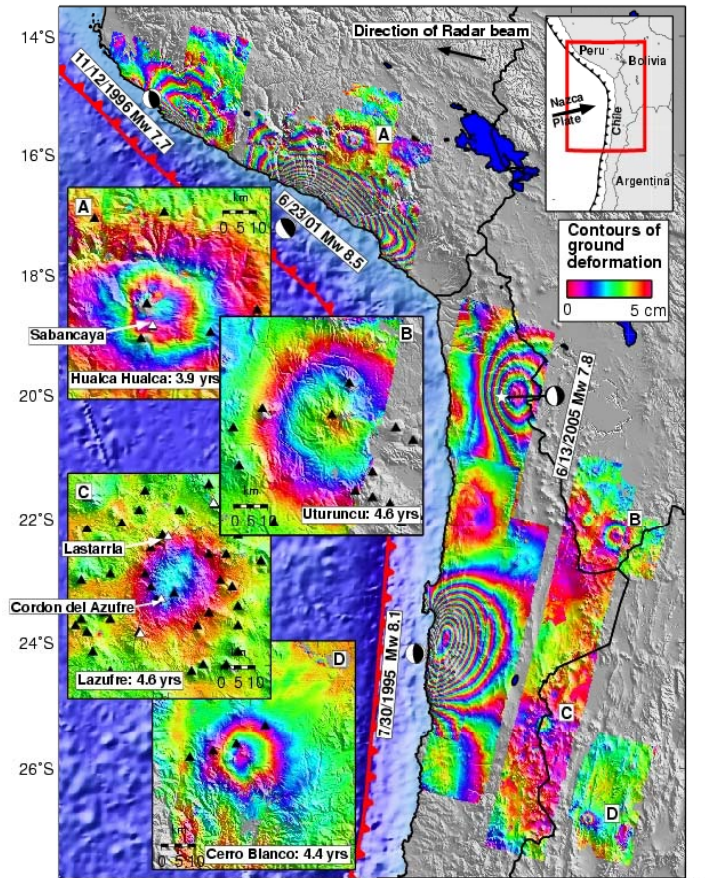


Chaitén volcano, Chile

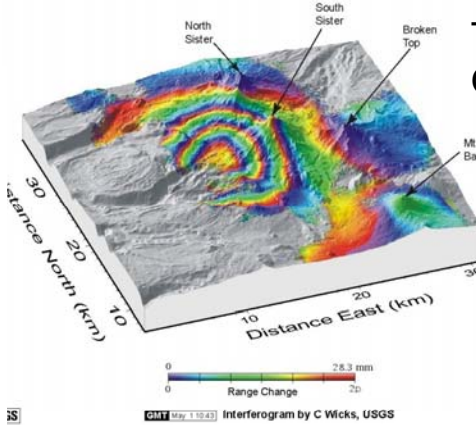
'Silent' volcano sources: Long time scales?

Central Andes

Courtesy M. Pritchard, Cornell Univ.

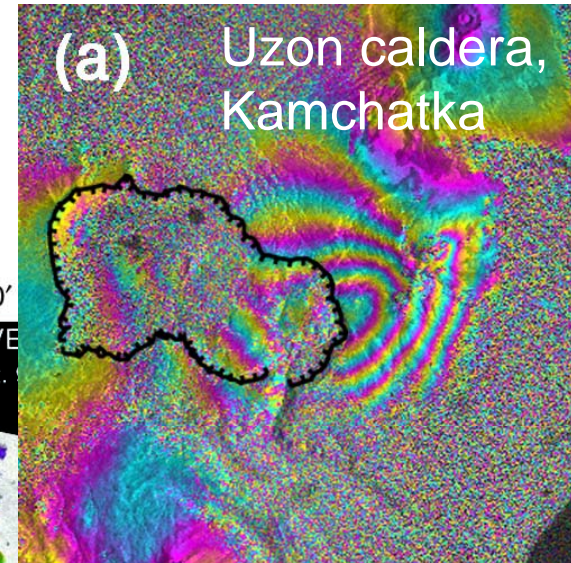


Pritchard and Simons, 2000

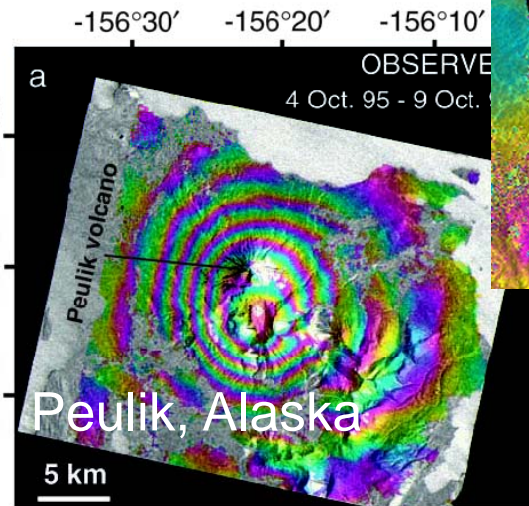


Three Sisters, Oregon

Courtesy C. Wicks, USGS



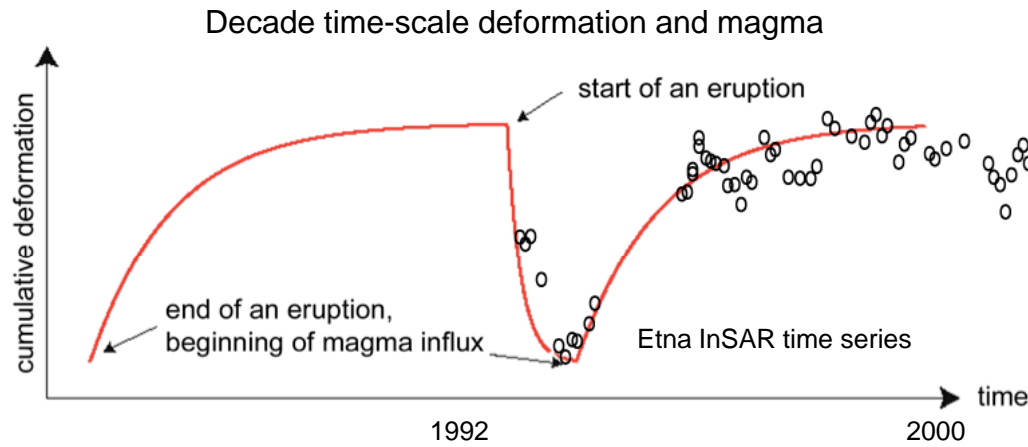
Lundgren and Lu, 2006



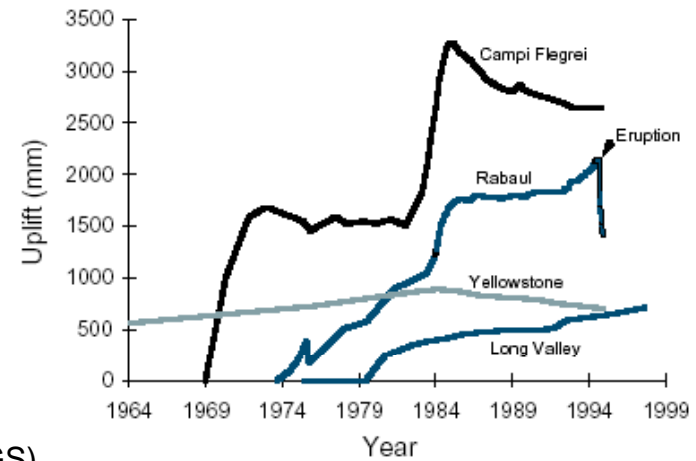
Lu et al., 2002

One of most exciting aspects of InSAR at volcanoes has been the discovery of deformation in unexpected places

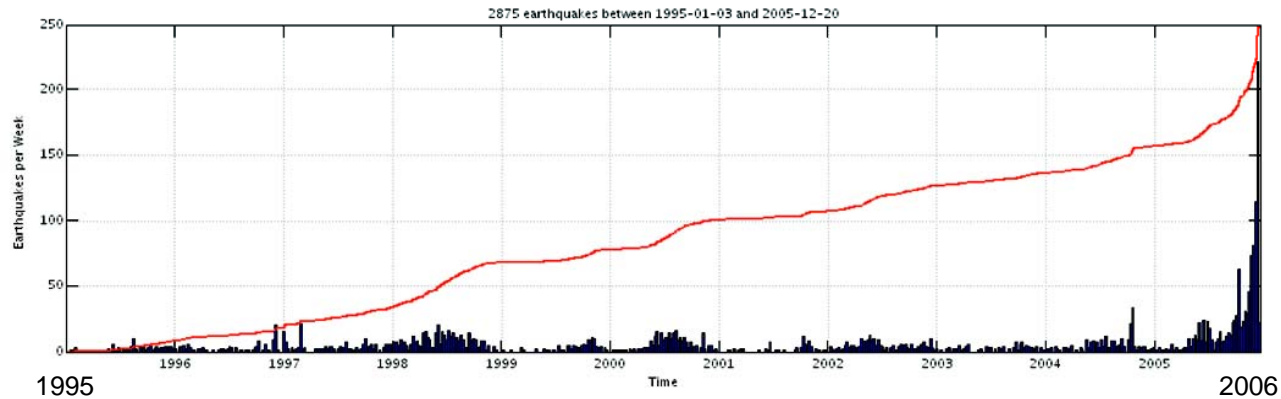
Longer term behavior



Caldera response times can be quite long with differing outcomes and mechanisms (Battaglia et al., 1999).



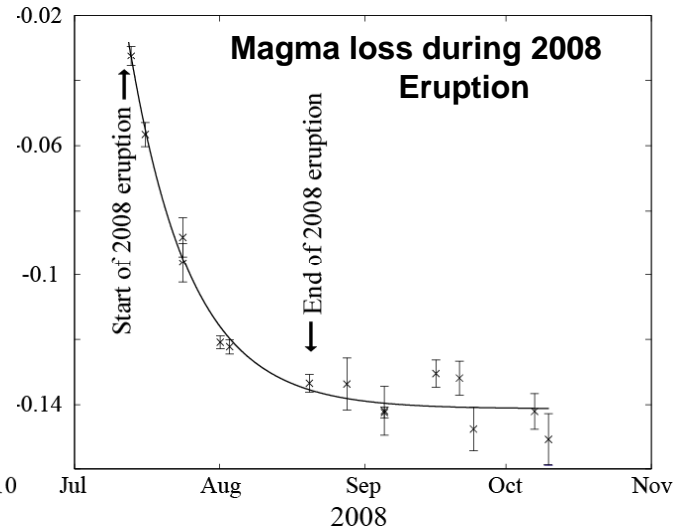
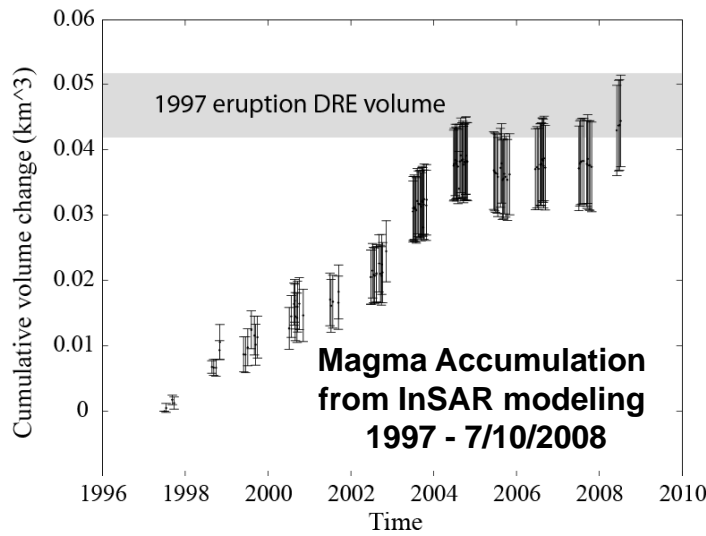
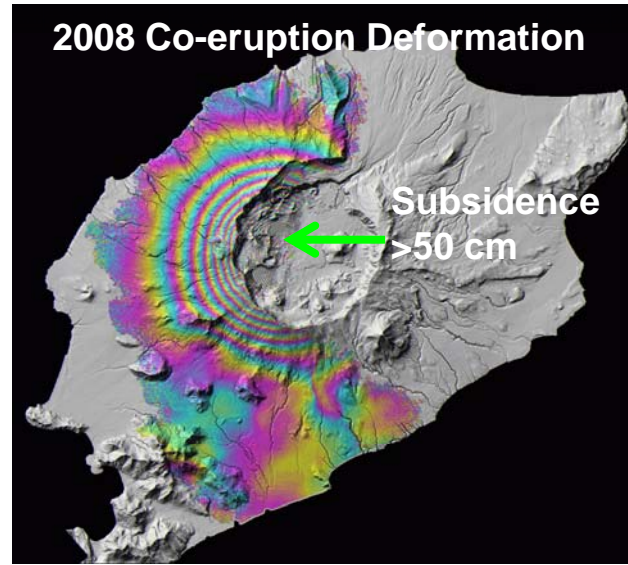
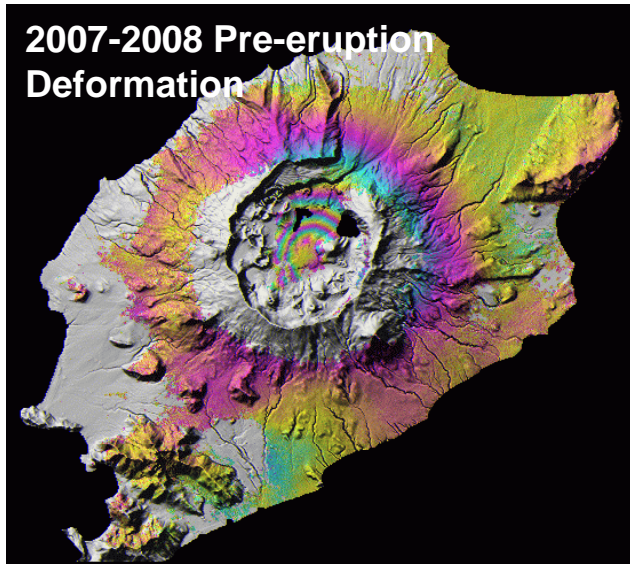
Augustine volcano 11 years of seismicity (USGS)



An aerial photograph showing a massive, billowing plume of white ash and steam rising from a volcanic eruption. The plume is dense and textured, with a bright sun visible in the upper left corner. The surrounding landscape is a vast, flat, light-colored plain, likely covered in ash or snow, with some distant mountain ranges visible under a clear blue sky.

Recent examples

Okmok eruption 2008
Preliminary results
courtesy Z. Lu, USGS





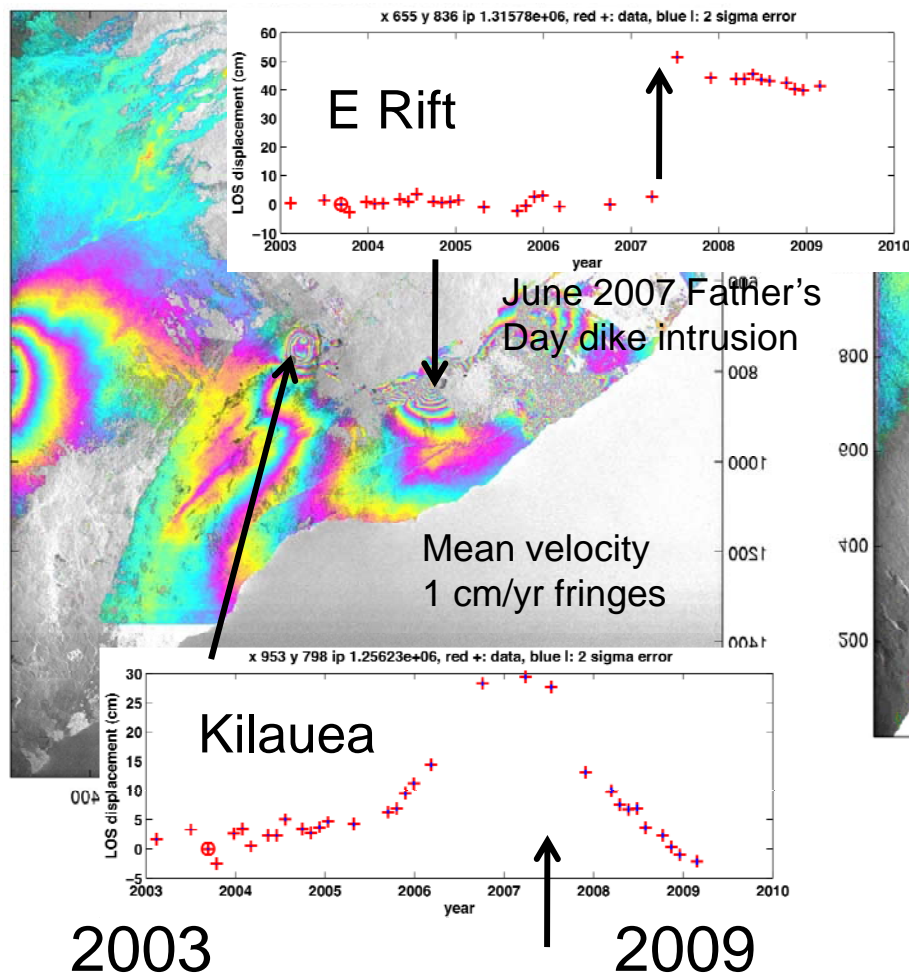
Kilauea

Complex deformation processes
before and after the June 2007
Father's Day event

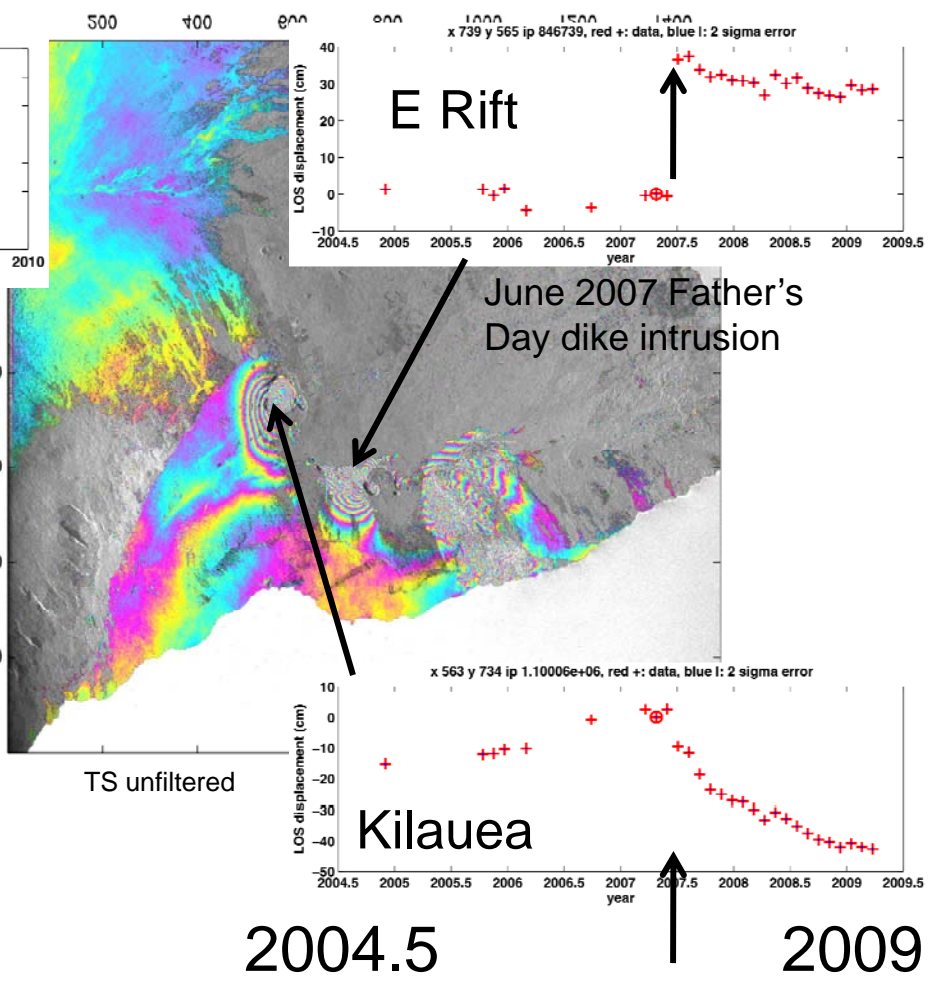
Kilauea Envisat time series inversion

ENVISAT T429_2

TS unfiltered



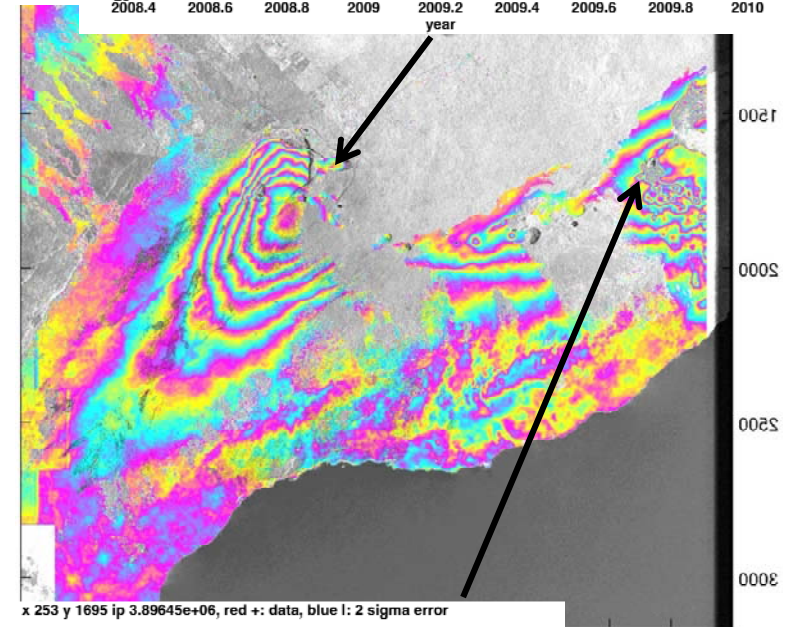
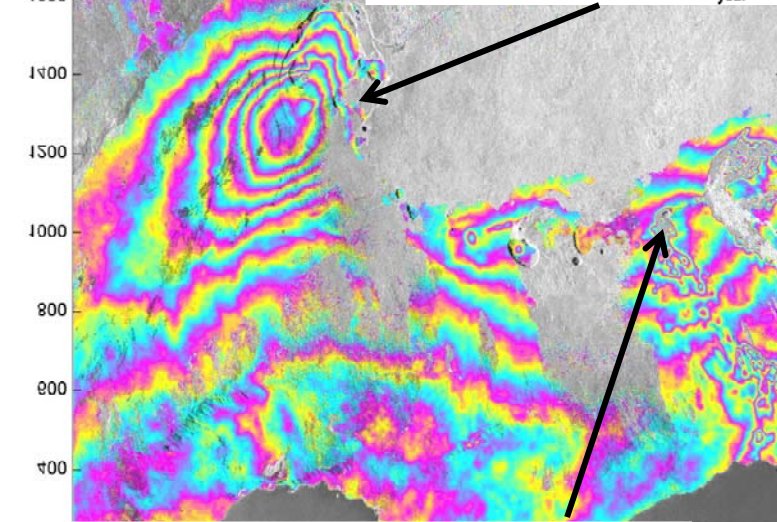
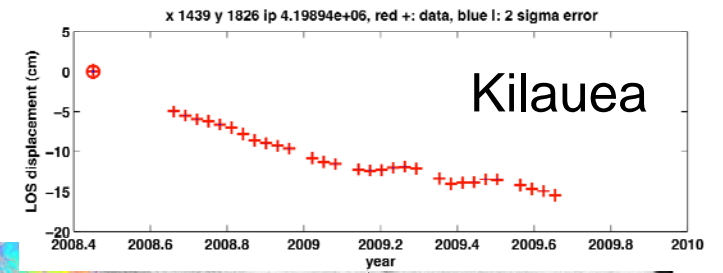
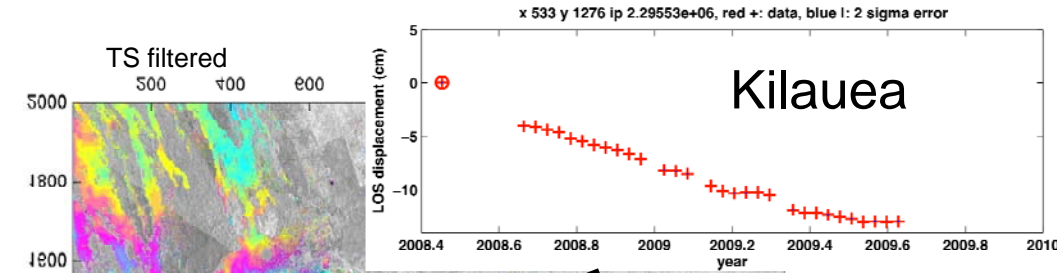
ENVISAT T322_1



June 2007 Father's Day dike intrusion

June 2007 Father's Day dike intrusion

Kilauea TSX time series analysis (2008-2009)

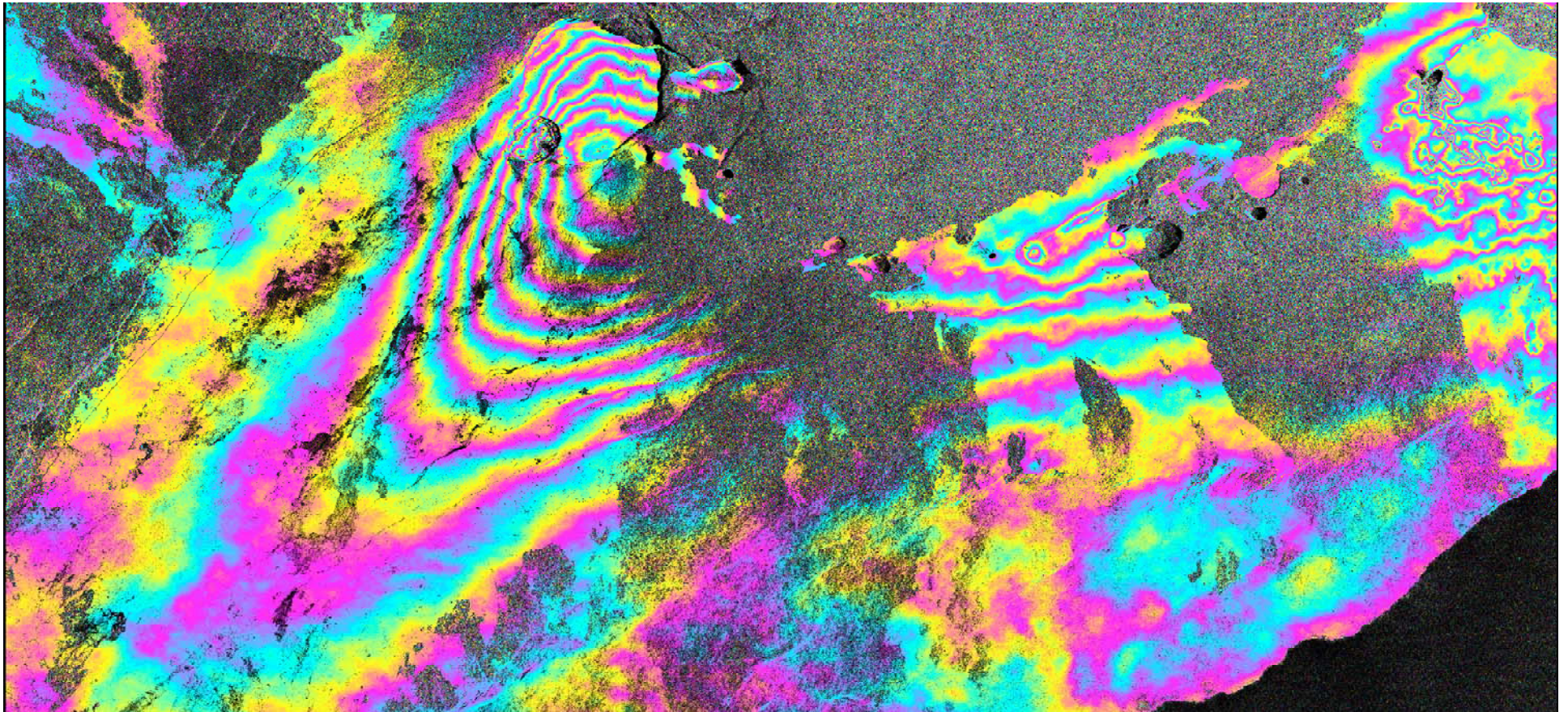


March 2009
increased activity

March 2009
increased activity



Kilauea TSX 1 year interferogram (2008.06.13 – 2009.07.03)



Unfiltered, 64 looks



Future trends

UAVSAR an airborne L-Band SAR for single and repeat pass interferometry

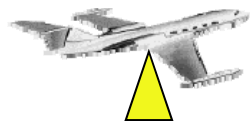


UAVSAR is ideally suited to making repeat pass observations of volcanic regions:

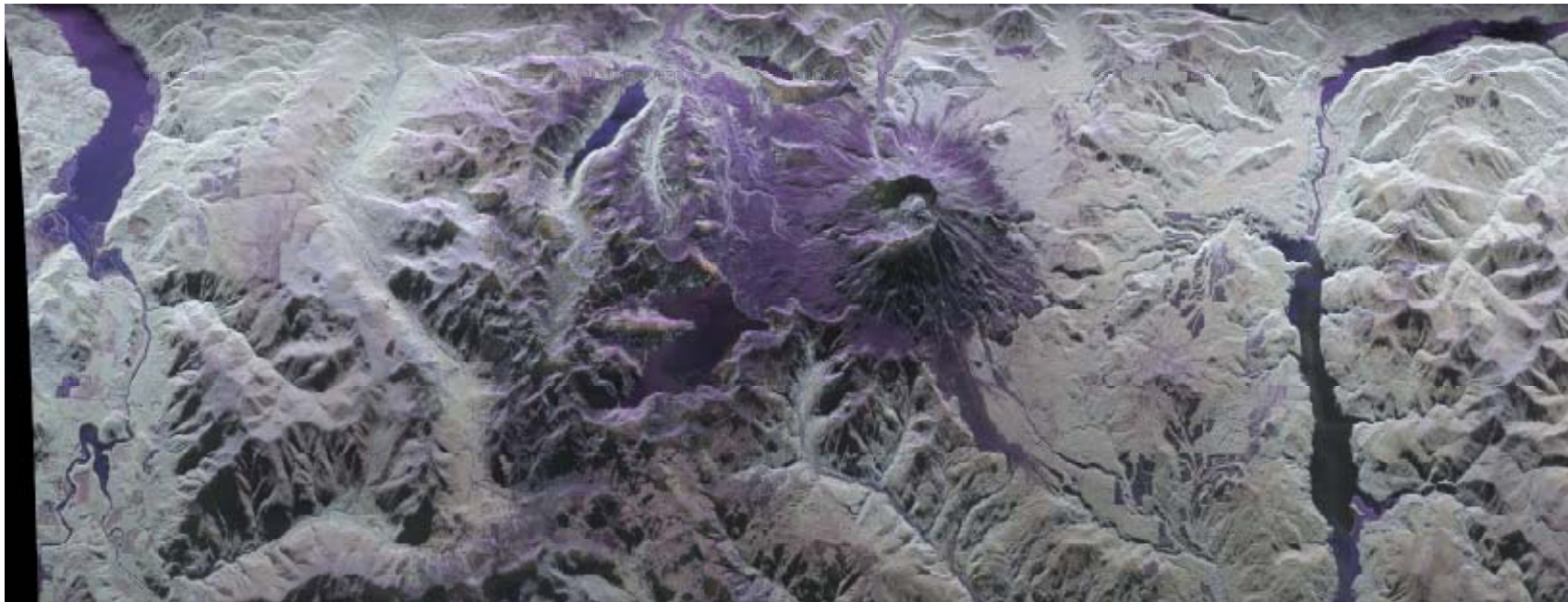
- Large swath (>20 km)
- fully polarimetric observations
- high altitude (> 12.5 km)
- Resolution: 1.6m range; 1m azimuth.
- L-band to reduce time decorrelation.
- Repeat observations on time scales as short as 20 minutes from any desired look direction.
- Flight path control to within a 10 m tube (usually within 5 m) and adjust its look direction electronically to compensate for aircraft attitude changes.
- Has a vector deformation capability.
- Can be rapidly deployed to monitor evolving volcano hazards or routinely tasked to monitor more quiescent volcanoes.

Mt St Helens - UAVSAR

March 24, 2008



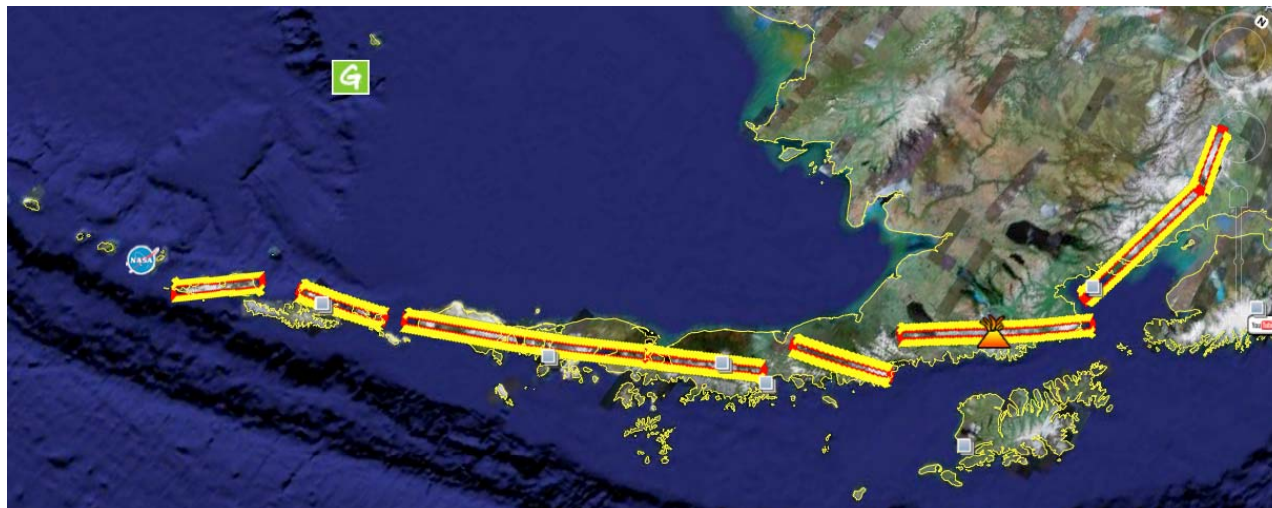
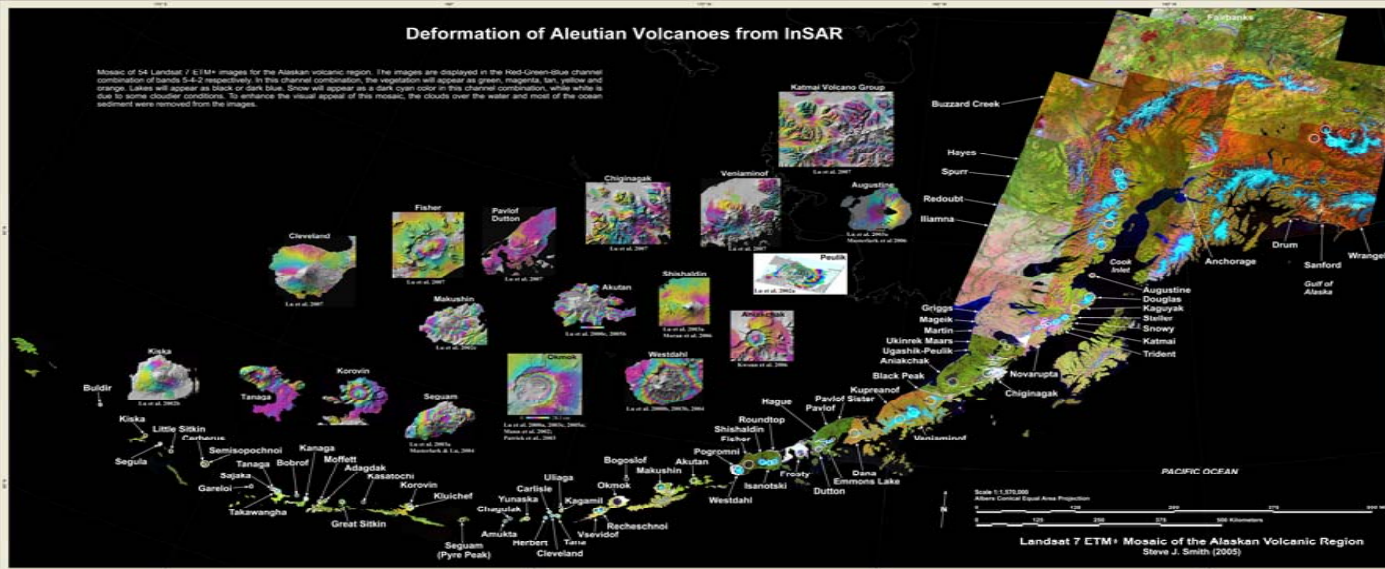
Flight
Direction



> 20 km

- Fully polarimetric image of Mt St Helens collected on March 24, 2008 by the UAVSAR radar. A second acquisition was collected on March 31, 2008.

UAVSAR Alaska measured July, Sept 2009



Lundgren, Lu, & Wicks



Conclusions

- InSAR is well known for its high spatial sampling and global coverage: => imaging of complex sources and new discoveries
- Future systems should improve many of these shortcomings
 - L-band to improve temporal correlation (ALOS-PALSAR, DESDynI)
 - Denser spatial sampling
 - UAVSAR, TSX, COSMO-SkyMed
 - Short repeat observations
 - 1 day or less for UAVSAR
 - 4 days? COSMO-SkyMed (X-band)
 - 8 days (tentative) DESDynI
 - 11 days TerraSAR-X (X-band)